Spectrochimica Acta Part A 71 (2009) 1944–1951

Contents lists available at ScienceDirect

Spectrochimica Acta Part A: Molecular and Biomolecular Spectroscopy

journal homepage: www.elsevier.com/locate/saa

A new family of Ru(II) polypyridyl complexes containing open-chain crown ether for Mg^{2+} and Ca^{2+} probing

Feixiang Cheng, Ning Tang*, Xing Yue

College of Chemistry and Chemical Engineering and State Key Laboratory of Applied Organic Chemistry, Lanzhou University, Lanzhou 730000, China

ARTICLE INFO

Article history:
Received 28 February 2008
Received in revised form 11 July 2008
Accepted 17 July 2008

Keywords:
Ru(II) complex
Open-chain crown ether
Photophysics
Electrochemistry
Cation-binding

ABSTRACT

Six polypyridyl bridging ligands BL^{1-6} containing open-chain crown ether, where BL^{1-3} formed by the condensation of 4,5-diazafluoren-9-hydrazine with 1,7-bis-(4-formylphenyl)-1,4,7-trioxaheptane, 1,10-bis-(4-formylphenyl)-1,4,7,10-tetraoxadecane, and 1,13-bis-(4-formylphenyl)-1,4,7,10,13-pentaoxatridecane, respectively, BL^{4-6} formed by the reaction of 9-(4-hydroxy)phenylimino-4,5-diazafluorene with diethylene glycol di-*p*-tosylate, triethylene glycol di-*p*-tosylate, and tetraethylene glycol di-*p*-tosylate, respectively, have been synthesized. Reaction of $Ru(bpy)_2Cl_2{\cdot}2H_2O$ with BL^{1-6}, respectively, afforded six bimetallic complexes $[(bpy)_2RuBL^{1-6}Ru(bpy)_2]^{4+}$ as PF_6^- salts. Cyclic voltammetry of these complexes is consistent with one Ru(II)-centered oxidation around 1.32 V and three ligand-centered reductions. These complexes show metal-to-ligand charge transfer absorption at 413–444 nm and emission at 570 nm. Binding behavior of complexes with alkali and alkaline-earth metal ions are investigated by UV–vis absorption, fluorescence, and cyclic voltammetry. Addition of alkali and alkaline-earth metal ions to the solution of $[(bpy)_2RuBL^{1-6}Ru(bpy)_2](PF_6)_4$ all result in a progressive quenching of fluorescence, a hyperchromic effect of UV–vis absorption, and a progressive cathodal shift of Ru(II)-centered $E_{1/2}$. Ru-BL^2 and Ru-BL^5 show the highest binding ability toward Mg^{2+} among the five cations examined while Ru-BL^3 and Ru-BL^6 exhibit good selective recognition ability to Ca^{2+}.

1. Introduction

There is currently a considerable effort devoted to the design and synthesis of ligands with recognition unit attached to a metal polypyridyl core. Properties of the metal polypyridyl complexes are modified by molecular level interactions between the recognition center and the substrate [1–4], so they are potentially useful in the preparation of chemical sensors. Chemosensors have drawn increasing attention for their use in fields as diverse as biology, medical analysis, environmental monitoring and so on [5–12]. Particular interest has been focused on the measurement of Mg^{2+} and Ca^{2+} in various systems, especially in biological materials, because alkaline-earth metal ion is the most abundant divalent cation in living cells, and plays vital roles in many cellular processes, for example, as an enzyme cofactor, stabilization of DNA conformation, ion transport through the membrane, maintenance of cell shape, and signal transduction. As a result, a great deal of effort has been devoted to the design and synthesis of sensitive and selective fluorescent sensors for Mg^{2+} and Ca^{2+} [13–19]. Ru(II) polypyridyl complexes have proved to be particularly versatile in sensor applications, because their emitting state energies and excited state redox properties are quite sensitive to external stimuli [20–30]. Herein, we report the synthesis and characterization of the six bridging ligands, their Ru(II) complexes, spectroscopic and electrochemical properties of these complexes in response to alkali and alkaline-earth metal ions binding.

2. Experimental

2.1. Materials

Solvents and raw materials were of analytical grade and were used as received. An exception was CH_3CN, which was filtered over activated alumina and distilled from P_2O_5 immediately prior to use. Tetrabutylammonium perchlorate (TBAP) [31], 4,5-diazafluoren-9-one (dafo) [32], 4,5-diazafluoren-9-hydrazine [33], diethylene glycol di-*p*-tosylate [34], triethylene glycol di-*p*-tosylate [34], tetraethylene glycol di-*p*-tosylate [34], 1,7-bis-(4-formylphenyl)-1,4,7-trioxaheptane [35], 1,10-bis-(4-formylphenyl)-1,4,7,10-tetraoxadecane [35], 1,13-bis-(4-formylphenyl)-1,4,7,10,13-pentaoxatridecane [35] and $Ru(bpy)_2Cl_2{\cdot}2H_2O$ [36] were synthesized according to the literature procedures.

* Corresponding author. Tel.: +86 931 8911218; fax: +86 931 8912582.
E-mail address: tangn@lzu.edu.cn (N. Tang).

1386-1425/$ – see front matter © 2008 Elsevier B.V. All rights reserved.
doi:10.1016/j.saa.2008.07.031

2.2. Physical measurements

Absorption spectra were obtained on a Varian Cary-100 UV–Visible spectrophotometer. ^{1}H NMR spectra were performed on a Mercury Plus 400 spectrometer using TMS as an internal standard. Elemental analyses were taken using a PerkinElmer 240C analytical instrument. ESI-HRMS was recorded on a Bruker Daltonics APEXII47e mass spectrometer. IR was obtained on a Nicolet 170SX FT-IR spectrophotometer as KBr discs. Electrochemical measurements were carried out at room temperature using a CHI 660B electrochemical workstation. Cyclic voltammetry and differential pulse voltammetry were obtained in CH_3CN and DMF by using a microcell equipped with a platinum disk working electrode, a platinum auxiliary electrode, and a saturated potassium chloride calomel with 0.1 M TBAP as supporting electrolyte. All samples were purged with nitrogen prior to measurement. Emission spectra were obtained in a 4:1 ethanol:methanol glass matrix at 77 K with a Hitachi F-4500 spectrophotometer. Emission quantum yields were calculated relative to $Ru(bpy)_3^{2+}$ (Φ_{std} = 0.376) in 4:1 ethanol:methanol [37].

3. Preparations

3.1. 1,7-Bis-(4-(4,5-diazafluoren-9-ylhydrazinyl)benzylidene)-1,4,7-trioxaheptane (BL^1)

A mixture of 1,7-bis-(4-formylphenyl)-1,4,7-trioxaheptane (64 mg, 0.20 mmol) and 4,5-diazafluoren-9-hydrazine (89 mg, 0.45 mmol) were refluxed for about 10 h in 10 mL ethanol containing a catalytic amount of acetic acid. Suspension formed after refluxing. The solution was hot filtered, and then washed with ethanol and diethyl ether affording the desired product as a yellow solid. Yield: 129 mg (95.6%). ^{1}H NMR (400 MHz, $CDCl_3$): δ 4.02 (t, J = 4.4 Hz, 4H), 4.29 (t, J = 4.4 Hz, 4H), 7.06 (d, J = 8.8 Hz, 4H), 7.31–7.36 (m, 4H), 7.88 (d, J = 8.8 Hz, 4H), 8.19 (d, J = 7.6 Hz, 2H), 8.62 (s, 2H), 8.73 (d, J = 3.6 Hz, 4H), 8.83 (d, J = 6.8 Hz, 2H). ESI-HRMS Found (Calcd.): m/z 671.2519 (671.2519) $(M+H)^+$, 693.2356 (693.2339) $(M+Na)^+$. IR (KBr): 1624.93, 1603.41, 1563.66, 1539.34, 1512.41, 1399.16, 1311.52, 1263.26, 1167.52, 1132.22, 1047.85, 1023.52, 824.96, 750.01 cm^{-1}.

3.2. 1,10-Bis-(4-(4,5-diazafluoren-9-ylhydrazinyl)benzylidene)-1,4,7,10-tetraoxadecane (BL^2)

BL^2 was prepared by the same procedure as that described for BL^1, except 1,10-bis-(4-formylphenyl)-1,4,7,10-tetraoxadecane (93 mg, 0.26 mmol) was used instead of 1,7-bis-(4-formylphenyl)-1,4,7-trioxaheptane to react with 4,5-diazafluoren-9-hydrazine (121 mg, 0.62 mmol). Yield: 175 mg (94.1%) of a yellow solid. ^{1}H NMR (400 MHz, $CDCl_3$): δ 3.81 (s, 4H), 3.94 (t, J = 4.4 Hz, 4H), 4.23 (t, J = 4.4 Hz, 4H), 7.04 (d, J = 8.0 Hz, 4H), 7.30–7.35 (m, 4H), 7.85 (d, J = 8.8 Hz, 4H), 8.17 (d, J = 8.0 Hz, 2H), 8.59 (s, 2H), 8.73 (d, J = 4.4 Hz, 4H), 8.82 (d, J = 8.0 Hz, 2H). ESI-HRMS Found (Calcd.): m/z 715.2776 (715.2781) $(M+H)^+$, 737.2631 (737.2601) $(M+Na)^+$. IR (KBr): 1627.14, 1603.73, 1563.75, 1542.53, 1512.09, 1398.47, 1309.69, 1256.22, 1169.67, 1114.77, 1021.78, 830.10, 753.10 cm^{-1}.

3.3. 1,13-Bis-(4-(4,5-diazafluoren-9-ylhydrazinyl)benzylidene)-1,4,7,10,13-pentaoxatridecane (BL^3)

BL^3 was prepared by the same procedure as that described for BL^1, except 1,13-bis-(4-formylphenyl)-1,4,7,10,13-pentaoxatridecane (165 mg, 0.41 mmol) was used instead of 1,7-bis-(4-formylphenyl)-1,4,7-trioxaheptane to react with 4,5-diazafluoren-9-hydrazine (197 mg, 1 mmol). Yield: 245 mg (78.5%) of a yellow solid. ^{1}H NMR (400 MHz, $CDCl_3$): δ 3.72 (t, J = 6.0 Hz, 4H), 3.76 (t, J = 6.0 Hz, 4H), 3.92 (t, J = 4.4 Hz, 4H), 4.21 (t, J = 4.4 Hz, 4H), 7.03 (d, J = 8.8 Hz, 4H), 7.29–7.35 (m, 4H), 7.84 (d, J = 8.8 Hz, 4H), 8.16 (d, J = 8.0 Hz, 2H), 8.58 (s, 2H), 8.72 (d, J = 4.4 Hz, 4H), 8.81 (d, J = 7.2 Hz, 2H). ESI-HRMS Found (Calcd.): m/z 759.3039 (759.3043) $(M+H)^+$, 781.2978 (781.2863) $(M+Na)^+$. IR (KBr): 1626.17, 1602.81, 1563.38, 1541.55, 1512.11, 1397.91, 1306.98, 1256.18, 1169.85, 1124.25, 1054.78, 1019.84, 829.94, 752.27 cm^{-1}.

3.4. 9-(4-Hydroxy)phenylimino-4,5-diazafluorene

A mixture of 4,5-diazafluoren-9-one (277 mg, 1.522 mmol) and 4-aminophenol (192 mg, 1.761 mmol) were refluxed for about 4 h in 20 mL ethanol containing a catalytic amount of acetic acid. After refluxing, a suspension formed. The solution was hot filtered, and then washed with ethanol and diethyl ether affording the desired product as a red solid. Yield: 311 mg (77.5%). ^{1}H NMR (400 MHz, DMSO-d_6): δ 6.87 (d, J = 6.4 Hz, 2H), 6.92 (d, J = 6.4 Hz, 2H), 7.13 (dd, J = 8.0, 1.6 Hz, 1H), 7.27 (dd, J = 8.0, 4.8 Hz, 1H), 7.54 (dd, J = 8.0, 4.8 Hz, 1H), 8.28 (dd, J = 8.0, 1.6 Hz, 1H), 8.67 (dd, J = 4.8, 1.6 Hz, 1H), 8.80 (dd, J = 4.8, 1.6 Hz, 1H), 9.54 (s, 1H).

3.5. 1,7-Bis-(4-(4,5-diazafluoren-9-ylimino)phenyl)-1,4,7-trioxaheptane (BL^4)

A mixture of diethylene glycol di-p-tosylate (113 mg, 0.272 mmol), 9-(4-hydroxy)phenylimino-4,5-diazafluorene (168 mg, 0.615 mmol) and K_2CO_3 (105 mg, 0.761 mmol) in 10 mL DMF were heated to 80 °C for 24 h under nitrogen atmosphere, then cooled down and poured the mixture into 200 mL water, a red precipitate was formed and collected by filtration. The resulting mixture was chromatographed on silica, eluting first with CH_2Cl_2/ethyl acetate 2:1 to remove impurities, then with CH_2Cl_2/CH_3CH_2OH 15:1 affording the desired product as a red solid. Yield: 99 mg (58.6%). ^{1}H NMR (400 MHz, $CDCl_3$): δ 4.03 (t, J = 4.8 Hz, 4H), 4.26 (t, J = 4.8 Hz, 4H), 6.93–7.06 (m, 12H), 7.39 (dd, J = 7.6, 4.8 Hz, 2H), 8.25 (dd, J = 8.0, 1.6 Hz, 2H), 8.65 (dd, J = 4.8, 1.6 Hz, 2H), 8.80 (dd, J = 5.2, 1.6 Hz, 2H). ESI-HRMS Found (Calcd.): m/z 617.2296 (617.2301) $(M+H)^+$, 639.2115 (639.2121) $(M+Na)^+$. IR (KBr): 1645.13, 1598.31, 1563.53, 1501.27, 1401.44, 1242.74, 1108.56, 835.92, 755.19 cm^{-1}.

3.6. 1,10-Bis-(4-(4,5-diazafluoren-9-ylimino)phenyl)-1,4,7,10-tetraoxadecane (BL^5)

BL^5 was prepared by the same procedure as that described for BL^4, except triethylene glycol di-p-tosylate (299 mg, 0.653 mmol) was used instead of diethylene glycol di-p-tosylate. Yield: 326 mg (75.3%) of a red solid. ^{1}H NMR (400 MHz, $CDCl_3$): δ 3.84 (s, 4H), 3.95 (t, J = 4.4 Hz, 4H), 4.23 (t, J = 4.4 Hz, 4H), 6.93–7.07 (m, 12H), 7.38 (dd, J = 8.0, 4.8 Hz, 2H), 8.23 (d, J = 7.2 Hz, 2H), 8.65 (d, J = 4.0 Hz, 2H), 8.79 (d, J = 5.2 Hz, 2H). ESI-HRMS Found (Calcd.): m/z 661.2555 (661.2563) $(M+H)^+$, 683.2468 (683.2383) $(M+Na)^+$. IR (KBr): 1648.65, 1597.61, 1562.91, 1501.41, 1400.82, 1243.83, 1108.97, 836.33, 755.43 cm^{-1}.

3.7. 1,13-Bis-(4-(4,5-diazafluoren-9-ylimino)phenyl)-1,4,7,10,13-pentaoxatridecane (BL^6)

BL^6 was prepared by the same procedure as that described for BL^4, except tetraethylene glycol di-*p*-tosylate (325 mg, 0.654 mmol) was used instead of diethylene glycol di-*p*-tosylate. Yield: 385 mg (84.8%) of a red solid. ^{1}H NMR (400 MHz, $CDCl_3$): 3.76 (t, J = 2.8 Hz, 4H), 3.80 (t, J = 2.8 Hz, 4H), 3.93 (t, J = 2.8 Hz, 4H), 4.20 (t, J = 2.8 Hz, 4H), 6.93–7.07 (m, 12H), 7.38 (dd, J = 7.2, 4.8 Hz, 2H), 8.22 (dd, J = 8.0, 1.6 Hz, 2H), 8.65 (d, J = 4.8 Hz, 2H), 8.79 (d, J = 5.2 Hz, 2H). ESI-HRMS Found (Calcd.): m/z 705.2815 (705.2825) $(M+H)^+$, 727.2661 (727.2645) $(M+Na)^+$. IR (KBr): 1650.58, 1598.19, 1563.20, 1502.62, 1401.85, 1244.34, 1108.31, 838.15, 755.47 cm^{-1}.

3.8. $[(bpy)_2RuBL^1Ru(bpy)_2](PF_6)_4$ ($Ru\text{-}BL^1$)

A mixture of BL^1 (52 mg, 0.078 mmol) and $Ru(bpy)_2Cl_2{\cdot}2H_2O$ (93 mg, 0.179 mmol) in 8 mL 2-methoxyethanol were heated to 115 °C for 12 h under nitrogen atmosphere. After cooling to room temperature, the solution was precipitated by dropwise addition of saturated aqueous NH_4PF_6 until no more precipitate formed. The solid was collected by filtration and washed with water, ethanol, followed by diethyl ether affording the crude product. The crude product was purified thrice by recrystallization from an acetonitrile–diethyl ether mixture (vapor diffusion method) giving a deep red solid. Yield: 110 mg (68.6%). ^{1}H NMR (400 MHz, DMSO-d_6): δ 3.90 (s, 4H), 4.29 (s, 4H), 7.19 (d, J = 8.0 Hz, 4H), 7.54–7.60 (m, 8H), 7.62 (d, J = 6.8 Hz, 2H), 7.65 (d, J = 7.6 Hz, 2H), 7.69 (d, J = 5.6 Hz, 2H), 7.73 (d, J = 5.2 Hz, 2H), 7.88 (d, J = 5.6 Hz, 4H), 8.10 (d, J = 8.0 Hz, 4H), 8.16–8.23 (m, 12H), 8.40 (t, J = 6.4 Hz, 2H), 8.82–8.86 (m, 10H), 8.97 (s, 2H). ESI-HRMS: m/z 894.1277 $(M-2PF_6)^{2+}$, 547.7628 $(M-3PF_6)^{3+}$. Elemental anal. Found: C, 46.25; H, 3.01; N, 10.79. Calcd. for $C_{80}H_{62}F_{24}N_{16}O_3P_4Ru_2$: C, 46.38; H, 3.11; N, 10.92. IR (KBr): 1634.60, 1604.25, 1538.23, 1512.85, 1466.27, 1422.59, 1313.52, 1259.99, 1172.67, 1121.64, 1028.81, 840.88, 763.88, 558.14 cm^{-1}.

3.9. $[(bpy)_2RuBL^2Ru(bpy)_2](PF_6)_4$ ($Ru\text{-}BL^2$)

$Ru\text{-}BL^2$ was prepared by the same procedure as that described for $Ru\text{-}BL^1$, except BL^2 (106 mg, 0.148 mmol) was used instead of BL^1 to react with $Ru(bpy)_2Cl_2{\cdot}2H_2O$ (178 mg, 0.342 mmol). Yield: 149 mg (47.5%) of a deep red solid. ^{1}H NMR (400 MHz, DMSO-d_6): δ 3.63 (s, 4H), 3.79 (s, 4H), 4.22 (s, 4H), 7.14 (d, J = 8.0 Hz, 4H), 7.51–7.58 (m, 8H), 7.60 (d, J = 4.4 Hz, 2H), 7.63 (d, J = 7.2 Hz, 2H), 7.67 (d, J = 5.2 Hz, 2H), 7.70 (d, J = 5.2 Hz, 2H), 7.85 (d, J = 5.2 Hz, 4H), 8.07 (d, J = 8.8 Hz, 4H), 8.13–8.20 (m, 12H), 8.36 (t, J = 6.8 Hz, 2H), 8.79–8.83 (m, 10H), 8.94 (s, 2H). ESI-HRMS m/z 916.1194 $(M-2PF_6)^{2+}$, 562.4444 $(M-3PF_6)^{3+}$. Elemental anal. Found: C, 46.42; H, 3.14; N, 10.56. Calcd. for $C_{82}H_{66}F_{24}N_{16}O_4P_4Ru_2$: C, 46.56; H, 3.32; N, 10.76. IR (KBr): 1631.25, 1603.85, 1538.26, 1512.23, 1465.46, 1422.35, 1312.56, 1258.86, 1172.15, 1121.68, 1028.36, 840.28, 764.16, 558.24 cm^{-1}.

3.10. $[(bpy)_2RuBL^3Ru(bpy)_2](PF_6)_4$ ($Ru\text{-}BL^3$)

$Ru\text{-}BL^3$ was prepared by the same procedure as that described for $Ru\text{-}BL^1$, except BL^3 (92 mg, 0.121 mmol) was used instead of BL^1 to react with $Ru(bpy)_2Cl_2{\cdot}2H_2O$ (143 mg, 0.275 mmol). Yield: 169 mg (64.1%) of a deep red solid. ^{1}H NMR (400 MHz, DMSO-d_6): δ 3.56 (s, 4H), 3.60 (s, 4H), 3.78 (s, 4H), 4.22 (s, 4H), 7.15 (d, J = 8.0 Hz, 4H), 7.52–7.58 (m, 8H), 7.60 (d, J = 4.4 Hz, 2H), 7.63 (d, J = 7.2 Hz, 2H), 7.67 (d, J = 4.8 Hz, 2H), 7.70 (d, J = 4.0 Hz, 2H), 7.86 (d, J = 5.6 Hz, 4H), 8.07 (d, J = 8.0 Hz, 4H), 8.14–8.20 (m, 12H), 8.37 (t, J = 7.2 Hz, 2H), 8.79–8.81 (m, 10H), 8.94 (s, 2H). ESI-HRMS m/z 938.1467 $(M-2PF_6)^{2+}$, 577.1124 $(M-3PF_6)^{3+}$. Elemental anal. Found: C, 46.59; H, 3.26; N, 10.35. Calcd. for $C_{84}H_{70}F_{24}N_{16}O_5P_4Ru_2$: C, 46.73; H, 3.44; N, 10.48. IR (KBr): 1629.14, 1603.12, 1537.16, 1512.68, 1465.44, 1421.85, 1311.91, 1258.45, 1171.65, 1121.62, 1028.08, 841.45, 764.80, 558.32 cm^{-1}.

3.11. $[(bpy)_2RuBL^4Ru(bpy)_2](PF_6)_4$ ($Ru\text{-}BL^4$)

A mixture of BL^4 (30 mg, 0.049 mmol) and $Ru(bpy)_2Cl_2{\cdot}2H_2O$ (58 mg, 0.112 mmol) in 15 mL 2-methoxyethanol was heated to 115 °C for 12 h under nitrogen atmosphere, then solvent was evaporated under reduced pressure, the residue was purified twice by column chromatography on alumina eluting first with CH_3CN/ethanol 10:1 to remove impurities, then with CH_3CN/ethanol 5:1 affording complex $[(bpy)_2RuBL^4Ru(bpy)_2]Cl_4$, which was then dissolved in a minimum amount of water followed by dropwise addition of saturated aqueous NH_4PF_6 until no more precipitate formed. This precipitate was purified by recrystallization from an acetonitrile–diethyl ether mixture (vapor diffusion method) giving a red solid. Yield: 66 mg (66.8%). ^{1}H NMR (400 MHz, DMSO-d_6): δ 3.86 (t, J = 4.4 Hz, 4H), 4.18 (t, J = 4.4 Hz, 4H), 7.10 (d, J = 8.8 Hz, 4H), 7.17 (d, J = 9.2 Hz, 4H), 7.26 (d, J = 8.0 Hz, 2H), 7.35 (dd, J = 7.6, 5.6 Hz, 2H), 7.49–7.63 (m, 12H), 7.73 (d, J = 5.6 Hz, 2H), 7.81 (d, J = 4.8 Hz, 2H), 7.84 (d, J = 5.2 Hz, 2H), 8.08 (d, J = 5.6 Hz, 2H), 8.11–8.21 (m, 10H), 8.42 (d, J = 7.2 Hz, 2H), 8.79 (d, J = 9.2 Hz, 4H), 8.83 (d, J = 9.2 Hz, 4H). ESI-HRMS: m/z 867.0982 $(M-2PF_6)^{2+}$, 529.4225 $(M-3PF_6)^{3+}$. Elemental anal. Found: C, 46.30; H, 2.99; N, 9.69. Calcd. for $C_{78}H_{60}F_{24}N_{14}O_3P_4Ru_2$: C, 46.40; H, 3.21; N, 9.82. IR (KBr): 1602.54, 1504.65, 1465.42, 1420.99, 1247.59, 1169.92, 1128.08, 1050.48, 839.98, 765.28, 558.76 cm^{-1}.

3.12. $[(bpy)_2RuBL^5Ru(bpy)_2](PF_6)_4$ ($Ru\text{-}BL^5$)

$Ru\text{-}BL^5$ was prepared by the same procedure as that described for $Ru\text{-}BL^4$, except BL^5 (51 mg, 0.077 mmol) was used instead of BL^4 to react with $Ru(bpy)_2Cl_2{\cdot}2H_2O$ (92 mg, 0.177 mmol).Yield: 58 mg (36.7%) of a red solid. ^{1}H NMR (400 MHz, DMSO-d_6): δ 3.65 (s, 4H), 3.79 (t, J = 4.4 Hz, 4H), 4.16 (t, J = 4.4 Hz, 4H),7.09 (d, J = 8.4 Hz, 4H), 7.17 (d, J = 9.2 Hz, 4H), 7.27 (d, J = 7.6 Hz, 2H), 7.36 (dd, J = 7.6, 5.6 Hz, 2H), 7.50–7.64 (m, 12H), 7.74 (d, J = 5.6 Hz, 2H), 7.82 (d, J = 6.0 Hz, 2H), 7.86 (d, J = 5.6 Hz, 2H), 8.09 (d, J = 5.6 Hz, 2H), 8.12–8.22 (m, 10H), 8.43 (d, J = 8.0 Hz, 2H), 8.80 (d, J = 8.8 Hz, 4H), 8.84 (d, J = 9.2 Hz, 4H). ESI-HRMS m/z 889.1290 $(M-2PF_6)^{2+}$, 544.4357 $(M-3PF_6)^{3+}$. Elemental anal. Found: C, 46.48; H, 3.12; N, 9.48. Calcd. for $C_{80}H_{64}F_{24}N_{14}O_4P_4Ru_2$: C, 46.62; H, 3.30; N, 9.72. IR (KBr): 1604.02, 1505.32, 1465.22, 1421.38, 1248.72, 1169.93, 1119.82, 1050.46, 840.95, 764.96, 558.51 cm^{-1}.

3.13. $[(bpy)_2RuBL^6Ru(bpy)_2](PF_6)_4$ ($Ru\text{-}BL^6$)

$Ru\text{-}BL^6$ was prepared by the same procedure as that described for $Ru\text{-}BL^4$, except BL^6 (50 mg, 0.071 mmol) was used instead of BL^4 to react with $Ru(bpy)_2Cl_2{\cdot}2H_2O$ (86 mg, 0.165 mmol).Yield: 93 mg (61.6%) of a red solid. ^{1}H NMR (400 MHz, DMSO-d_6): δ 3.58 (t, J = 2.8 Hz, 4H), 3.62 (t, J = 2.8 Hz, 4H), 3.79 (t, J = 4.4 Hz, 4H), 4.16 (t, J = 4.4 Hz, 4H),7.11 (d, J = 8.4 Hz, 4H), 7.19 (d, J = 8.8 Hz, 4H), 7.29 (d, J = 7.6 Hz, 2H), 7.38 (dd, J = 7.6, 6.0 Hz, 2H), 7.51–7.65 (m, 12H), 7.76 (d, J = 5.2 Hz, 2H), 7.83 (d, J = 5.2 Hz, 2H), 7.87 (d, J = 5.6 Hz, 2H), 8.10 (d, J = 5.6 Hz, 2H), 8.14–8.24 (m, 10H), 8.45 (d, J = 8.0 Hz, 2H), 8.82 (d, J = 8.8 Hz, 4H), 8.86 (d, J = 8.8 Hz, 4H). ESI-HRMS m/z 911.1359 $(M-2PF_6)^{2+}$, 559.1691 $(M-3PF_6)^{3+}$. Elemental anal. Found: C, 46.64; H, 3.25; N, 9.29. Calcd. for $C_{82}H_{68}F_{24}N_{14}O_5P_4Ru_2$: C, 46.48; H, 3.40; N, 9.63. IR (KBr): 1602.29,

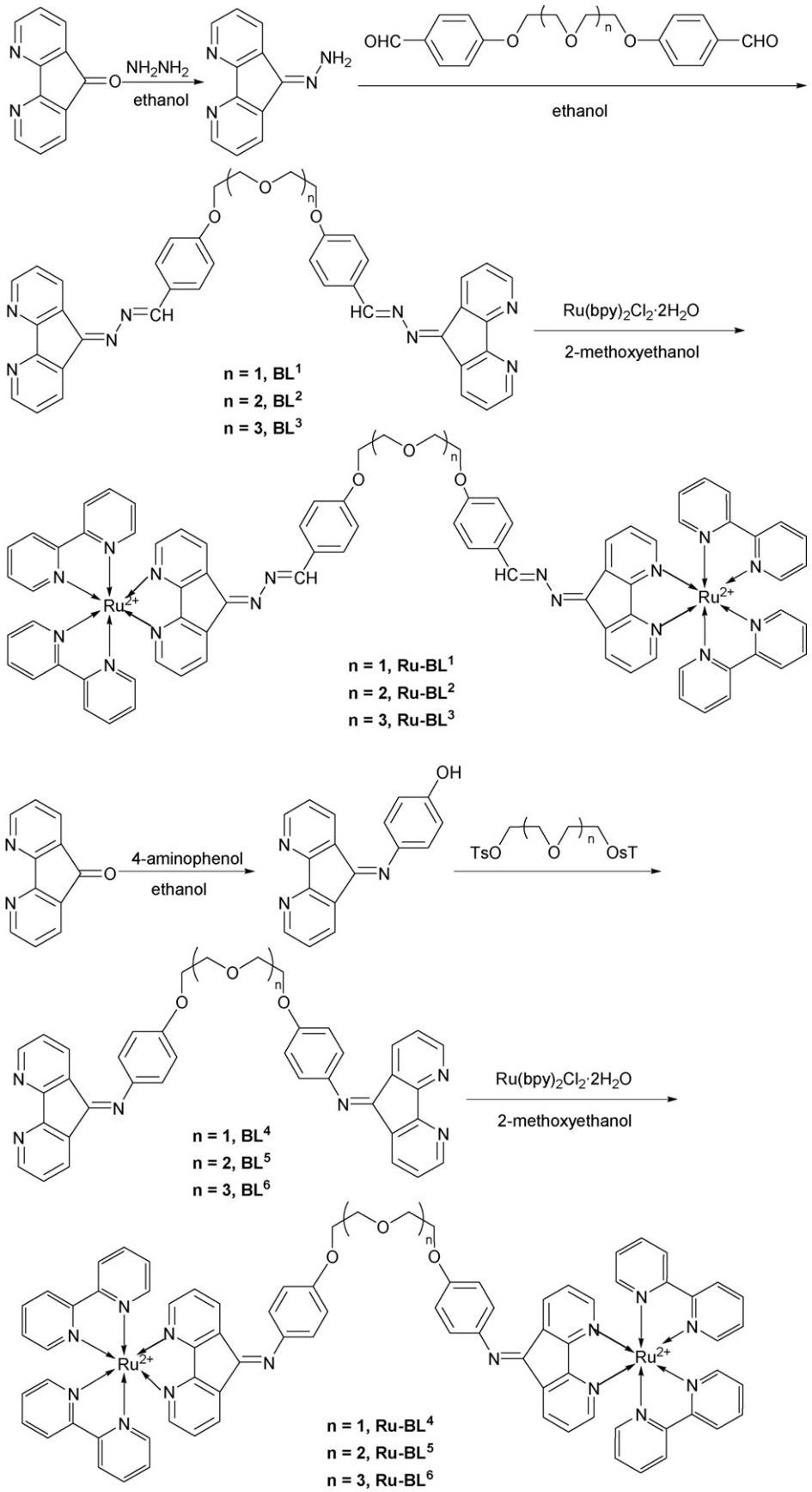

Scheme 1. Synthesis of bridging ligands BL^{1-6} and corresponding complexes Ru-BL^{1-6}.

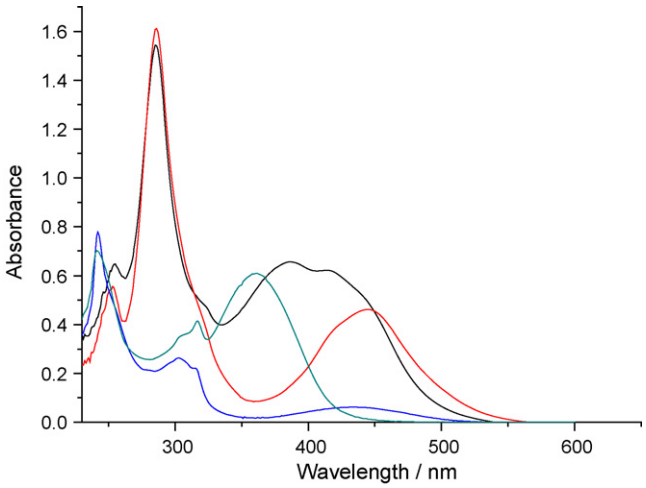

Fig. 1. UV–vis absorption spectra of BL^1 (10^{-5} M, dark cyan, typical for BL^{1-3}) and BL^4 (10^{-5} M, blue, typical for BL^{4-6}) in $CHCl_3$ at room temperature, Ru-BL^1 (10^{-5} M, black, typical for Ru-BL^{1-3}) and Ru-BL^4 (10^{-5} M, red, typical for Ru-BL^{4-6}) in CH_3CN at room temperature. (For interpretation of the references to colour in this figure legend, the reader is referred to the web version of the article.)

1504.41, 1465.85, 1421.17, 1248.53, 1169.07, 1115.95, 1059.39, 841.01, 764.92, 558.35 cm^{-1}.

4. Results and discussion

4.1. Synthesis

The outline of the synthesis of the previously unreported six bridging ligands BL^{1-6} and corresponding Ru(II) complexes $[(bpy)_2RuBL^{1-6}Ru(bpy)_2](PF_6)_4$ is presented in Scheme 1. Preparation of the ligands BL^{1-3} was a Schiff-base formation from the condensation of 4,5-diazafluoren-9-hydrazine with 1,7-bis-(4-formylphenyl)-1,4,7-trioxaheptane, 1,10-bis-(4-formylphenyl)-1,4,7,10-tetraoxadecane, and 1,13-bis-(4-formylphenyl)-1,4,7,10,13-pentaoxatridecane, respectively. Intermediate 9-(4-hydroxy)phenylimino-4,5-diazafluorene was prepared by a modified procedure [38]. BL^{4-6} were prepared by reaction of 9-(4-hydroxy)phenylimino-4,5-diazafluorene with diethylene glycol di-*p*-tosylate, triethylene glycol di-*p*-tosylate, and tetraethylene glycol di-*p*-tosylate, respectively.

For each of the ligands, Ru(II) complex was prepared under nitrogen atmosphere by heating the starting materials in 2-methoxyethanol. The resulting complexes were characterized by ^1H NMR, ESI-HRMS, elemental analysis and IR.

Table 1
UV–vis absorption data of ligands and corresponding Ru(II) polypyridyl complexes[a]

λ_{max} (nm) ($10^4\varepsilon$, M^{-1} cm^{-1})				
BL^1	361 (6.10)	317 (4.15)	241 (7.01)	
BL^2	361 (6.26)	317 (4.27)	242 (6.95)	
BL^3	361 (6.27)	317 (4.21)	241 (6.97)	
BL^4	430 (0.62)	302 (2.63)	241 (7.78)	
BL^5	430 (0.64)	302 (2.75)	241 (8.19)	
BL^6	430 (0.64)	302 (2.68)	241 (7.92)	
Ru-BL^1	413 (6.23)	386 (6.57)	285 (15.43)	255 (6.49)
Ru-BL^2	413 (6.10)	386 (6.30)	286 (15.11)	255 (6.58)
Ru-BL^3	413 (6.77)	386 (7.08)	286 (16.39)	255 (6.96)
Ru-BL^4	444 (4.62)		286 (16.12)	253 (5.57)
Ru-BL^5	444 (4.21)		286 (14.68)	252 (5.17)
Ru-BL^6	444 (4.49)		286 (15.62)	252 (5.55)

[a] All ligand samples were measured in $CHCl_3$ solution at room temperature, all complex samples were measured in CH_3CN solution at room temperature.

4.2. Absorption spectra

Absorption spectra of the six ligands have been studied in $CHCl_3$, and the corresponding six complexes studied in CH_3CN. Working concentration of all samples is 10^{-5} M. The spectra are shown in Fig. 1 with the data summarized in Table 1. Absorption bands of the ligands can be assigned to ligand-centered intraligand $\pi \rightarrow \pi^*$ or $n \rightarrow \pi^*$ transitions. Assignments of the absorption bands are made on the basis of the well-documented optical transitions of other Ru(II) polypyridyl complexes [39–44]. For complexes Ru-BL^{1-3}, absorption bands at around 255 and 286 nm region are attributed to the intraligand $\pi \rightarrow \pi^*$ transitions centered on the bipyridine. Peak observed around 386 nm can be assigned to ligands BL^{1-3} centered intraligand $\pi \rightarrow \pi^*$ transitions. With reference to previous spectroscopic studies of Ru(II) complexes with similar diimine ligands [45–47], ligands BL^{1-3} have strong π acceptor capacity due to the large π conjugated framework, which results in a greater effective nuclear charge on ruthenium. This factor stabilizes the $d\pi$ orbital of Ru(II). So, the bands at 413 nm are assigned to $d\pi(Ru) \rightarrow \pi^*(BL^{1-3})$ transitions.

Absorption spectra of complexes Ru-BL^{4-6} comprise three distinct regions. Bands at around 252 and 286 nm are also attributed to the bipyridine centered intraligand $\pi \rightarrow \pi^*$ transitions. The strong band at 444 nm is assigned to admixture of the $d\pi(Ru) \rightarrow \pi^*(bpy)$ and $d\pi(Ru) \rightarrow \pi^*(BL^{4-6})$. The MLCT absorption maximum is blue-shifted by 6 nm compared with $Ru(bpy)_3^{2+}$ [48], which shows the donor property of BL^{4-6} is weaker than that of bipyridine.

4.3. Electrochemistry

Electrochemical behaviors of complexes have been studied in CH_3CN and in DMF. In CH_3CN, the reductions are not well behaved,

Table 2
Electrochemical and fluorescence data of Ru(II) polypyridyl complexes

Complex	$E_{1/2}$ (V) (ΔE_p, mV)[a]				Emission[b]	
	Oxidation		Reduction		λ_{max} (nm)	Φ
Ru-BL^1	1.30 (122)	−0.69 (252)	−1.36 (131)	−1.63 (96)	571	0.039
Ru-BL^2	1.31 (130)	−0.69 (238)	−1.35 (122)	−1.61 (82)	571	0.034
Ru-BL^3	1.30 (127)	−0.69 (247)	−1.35 (117)	−1.61 (84)	570	0.028
Ru-BL^4	1.35 (146)	-0.78^{irr}	−1.37 (119)	−1.63 (74)	570	0.012
Ru-BL^5	1.36 (145)	-0.80^{irr}	−1.38 (117)	−1.64 (71)	571	0.011
Ru-BL^6	1.36 (145)	-0.79^{irr}	−1.38 (113)	−1.64 (76)	571	0.010

[a] Oxidation potentials recorded in 0.1 M TBAP/CH_3CN, reduction potentials recorded in 0.1 M TBAP/DMF and potentials were given versus SCE; scan rate = 200 mV/s.
[b] All samples were measured at 77 K in 4:1 ethanol:methanol glassy matrix.

$$[(bpy)_2Ru^{II}BLRu^{II}(bpy)_2]^{4+} + 2e^- = [(bpy)_2Ru^{II}BL^{2-}Ru^{II}(bpy)_2]^{2+}$$

$$[(bpy)_2Ru^{II}BL^{2-}Ru^{II}(bpy)_2]^{2+} + 2e^- = [(bpy)(bpy^{-})Ru^{II}BL^{2-}Ru^{II}(bpy^{-})(bpy)]$$

$$[(bpy)(bpy^{-})Ru^{II}BL^{2-}Ru^{II}(bpy^{-})(bpy)] + 2e^- = [(bpy^{-})(bpy^{-})Ru^{II}BL^{2-}Ru^{II}(bpy^{-})(bpy^{-})]^{2-}$$

Scheme 2. Reduction processes of bimetallic complex Ru-BL[1].

probably due to the adsorption of the reduced species onto the surface of the platinum electrode. In DMF, the complexes display three reduction processes, but do not show the oxidative waves due to the limitation by the solvent. Therefore, the oxidation potentials recorded in CH_3CN, but the reduction potentials recorded in DMF (Table 2).

Cyclic voltammetry of complex Ru-BL[1] exhibits a Ru(II)-based oxidation at 1.30 V. Compared with $[(bpy)_2Ru(dafo)](PF_6)_2$ [40], which can be regarded as parent complex, this oxidation potential is slightly more negative (by about 90 mV), which indicates that bridging ligand BL[1] is less acidic than dafo. In the current study, bimetallic complex Ru-BL[1] shows a single, unperturbed wave in cyclic voltammetry and a single peak without broadening in differential pulse voltammetry. A two-electron process for each couple of complexes Ru-BL[1–6] was confirmed by coulometry. So, this oxidation can be ascribed to a two-electron quasi-reversible process.

Reduction at around −0.69 V is a quasi-reversible process associated with the BL[1], this is consistent with the addition of electrons to the low energy LUMO mainly localized on the BL[1] giving complex $[(bpy)_2Ru^{II}BL^{2-}Ru^{II}(bpy)_2]^{2+}$. Compared with the uncoordinated ligand BL[1] (−1.06 V, a two-electron quasi-reversible process in DMF), the potential shifts positively about 0.4 V due to the presence of the positively charged ruthenium centers. The second reduction at −1.37 V is located on one of the two bpy ligands on each metallic terminal, adding electrons to the bpy localized LUMO+1 giving the species $[(bpy)(bpy^{\bullet-})Ru^{II}BL^{2-}Ru^{II}(bpy^{\bullet-})(bpy)]$. Just as the oxidation, the reductions of the remote bpy appear at the same potential, indicating no interaction between the two sites. The third reduction appearing at −1.75 V is reversible and yields the species $[(bpy^{\bullet-})(bpy^{\bullet-})Ru^{II}BL^{2-}Ru^{II}(bpy^{\bullet-})(bpy^{\bullet-})]^{2-}$. Reduction processes of bimetallic complexes Ru-BL[1] are presented in Scheme 2. Electrochemistry behaviors of complex Ru-BL[2–6] are the same as Ru-BL[1] except the first reduction wave of Ru-BL[4–6] is irreversible.

4.4. Fluorescence behaviors

Emission band maxima and emission quantum yields of the Ru(II) complexes are summarized in Table 2. Upon excitation into the MLCT band of the complexes, they are non-emissive in CH_3CN at room temperature, but they display vibrational components similar to that of $Ru(bpy)_3^{2+}$ at 77 K in 4:1 EtOH:MeOH glassy matrix [49]. Cherry and co-workers [50] have reported crisply that such mixed imine Ru(II) complexes were poor emitters at room temperature. Complexes Ru-BL[1–6] exhibit their characteristic emission at around 570 nm in 4:1 EtOH:MeOH glassy matrix at 77 K.

4.5. Cation binding

It is known that the conformation of noncyclic crown ether changes drastically from a linear structure to a pseudocyclic structure upon complex interaction with alkali or alkaline-earth metal ions. So, the six complexes have been designed to bind adventitious Li^+, Na^+, Mg^{2+}, Ca^{2+} or Ba^{2+} using the recognition site.

When Li^+, Na^+, Mg^{2+}, Ca^{2+} and Ba^{2+} were added to the solution of Ru-BL[1–6], it was found that addition of a large excess of alkali and alkaline-earth metal ions barely perturb the fluorescence spectra of Ru-BL[1] and Ru-BL[4]. Emission spectrum of Ru-BL[2], Ru-BL[3], Ru-BL[5], and Ru-BL[6] underwent a progressive decrease in relative fluorescence intensity that was [M] dependent, but no shift of emission band maxima was observed. The five cations quench the fluorescence of Ru-BL[2] (Fig. 2) and Ru-BL[5] in the order of $Mg^{2+} > Ca^{2+} > Ba^{2+} > Li^+ > Na^+$, quench the fluorescence of Ru-BL[3] and Ru-BL[6] in the order of $Ca^{2+} > Mg^{2+} > Ba^{2+} > Na^+ > Li^+$ (Table 3). Fluorescence quenching can be ascribed to binding of the cation to the pseudocyclic polyether cavity, the environment around the Ru(II) polypyridyl complex chromophore has been perturbed. Among the complexes Ru-BL[1–6], Mg^{2+} cation-induced fluorescence quenching of Ru-BL[5] and Ca^{2+} cation-induced fluorescence quenching of Ru-BL[6] are interesting, because the fluorescence quenching reached as high as 78% for Ru-BL[5] and 63% for Ru-BL[6].

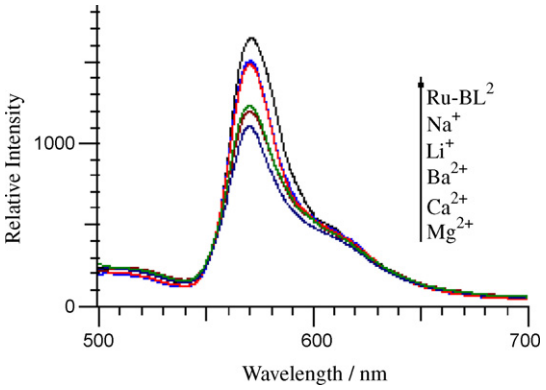

Fig. 2. Fluorescence spectra of Ru-BL[2] (10^{-5} M) in the presence of Mg^{2+}, Ca^{2+}, Ba^{2+}, Li^+, and Na^+ (10^{-3} M) at 77 K in 4:1 EtOH:MeOH glassy matrix. (For interpretation of the references to colour in this figure legend, the reader is referred to the web version of the article.)

Cation binding studies of Ru-BL[1–6] have been pursued further using UV–vis absorption. It was found that Li^+ and Na^+ have little effect on the UV–vis absorption of Ru-BL[1–6], and addition of a large excess of alkali and alkaline-earth metal ions to the CH_3CN solution of complexes barely perturb the UV–vis absorption spectra of Ru-BL[1] and Ru-BL[4].

UV–vis absorption spectra tracing upon sequential addition of Ca^{2+} to the CH_3CN solution of Ru-BL[6] is shown in Fig. 3. A summary of the titration curves monitoring the changes in absorbance at 444 nm of Ru-BL[6] in CH_3CN versus the concentration of Mg^{2+}, Ca^{2+} and Ba^{2+} is depicted in Fig. 4. The curves show a gradual increase in absorbance at ^{1}MLCT band upon increasing the cation concentration, reaching saturation at higher cation concentrations. With such absorption information, the binding constants could be determined with Eq. (1), where A_0 is the initial absorbance in the

Table 3
I/I_0 and stability constant K_s of Ru(II) polypyridyl complexes upon the addition of Li^+, Na^+, Mg^{2+}, Ca^{2+} and Ba^{2+}[a]

	I/I_0[b] (stability constant K_s[c])				
	Li^+	Na^+	Mg^{2+}	Ca^{2+}	Ba^{2+}
Ru-BL[2]	0.90 (−)	0.91 (−)	0.79 (852)	0.86 (473)	0.87 (262)
Ru-BL[3]	0.91(−)	0.88 (−)	0.85 (392)	0.82 (968)	0.87 (275)
Ru-BL[5]	0.70 (−)	0.83 (−)	0.22 (1921)	0.29 (926)	0.61 (258)
Ru-BL[6]	0.89 (−)	0.87 (−)	0.52 (776)	0.37 (1682)	0.72 (398)

[a] [M] = 10^{-5} M; [Ru-BL[2,3,5,6]] = 10^{-3} M.
[b] In 4:1 EtOH:MeOH glassy matrix at 77 K.
[c] In CH_3CN at room temperature. (−) Change of UV–vis absorption intensity is too small to calculate.

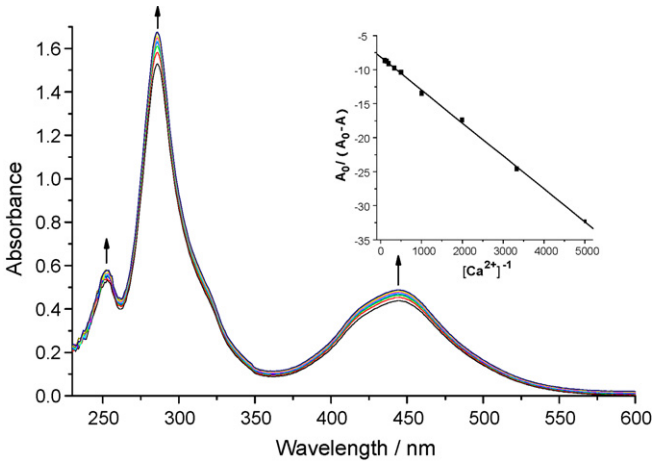

Fig. 3. UV–vis spectra of Ru-BL^6 (10^{-5} M) in CH_3CN solution upon increasing the concentration of Ca^{2+}; plotting $A_0/(A_0-A)$ at 444 nm versus $[Ca^{2+}]^{-1}$ at 444 nm (inset). (For interpretation of the references to colour in the artwork, the reader is referred to the web version of the article.)

absence of metal cations, A is the absorbance of the solution mixture at an alkaline-earth metal ion concentration $[M^{2+}]$, ε_f and ε_b are the molar absorption coefficients of the host complexes and the bound species, respectively, and K_s is the binding constant. Plotting $A_0/(A_0-A)$ versus $[M^{2+}]^{-1}$ gave a satisfactory straight line and the binding constant can be determined from the ratio of the y-intercept/slope. Plotting of $A_0/(A_0-A)$ at 444 nm versus $[Ca^{2+}]^{-1}$ of Ru-BL^6 give a satisfactory straight line (Fig. 3), and the binding constant of complex Ru-BL^6 to bind Ca^{2+} is 1682. Using the same method, the binding constants of Mg^{2+} and Ba^{2+} are calculated to be 776 and 398, respectively. Ru-BL^6 shows the highest binding ability toward Ca^{2+} among five cations examined, and the relative selectivity for Ca^{2+} is about 2 times of Mg^{2+}, and over four times of Ba^{2+}.

$$\frac{A_0}{(A_0-A)} = \left[\frac{\varepsilon_f}{(\varepsilon_f-\varepsilon_b)}\right]\left(1+\frac{1}{K_s[M]}\right) \quad (1)$$

Behaviors of the analogues Ru-BL^2, Ru-BL^3 and Ru-BL^5 are examined for comparison. Binding constants are collected in Table 3. Behavior observed for Ru-BL^3 is similar to that of Ru-BL^6, which shows the selectivity for Ca^{2+} among the five cations examined. Inspection of Table 3 reveals that Ru-BL^2 and Ru-BL^5 shows the highest binding ability toward Mg^{2+} among the five cations examined. Ru-BL^2 and Ru-BL^5, both including four oxygen atoms in the open-chain crown ether unit, capture Mg^{2+}, Ca^{2+}, and Ba^{2+} in the order: $Mg^{2+} > Ca^{2+} > Ba^{2+}$. Ru-BL^3 and Ru-BL^6, which contain five oxygen atoms in the open-chain crown ether unit, capture Mg^{2+}, Ca^{2+}, and Ba^{2+} in the order: $Ca^{2+} > Mg^{2+} > Ba^{2+}$. This order is consistent with the sequence of fluorescence quenching.

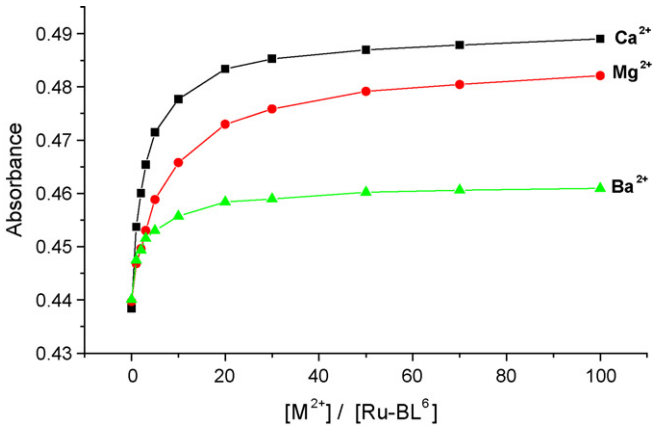

Fig. 4. UV–vis titration curves of complex Ru-BL^6 with Mg^{2+}, Ca^{2+} and Ba^{2+} in CH_3CN at room temperature. The absorbance was monitored at 444 nm.

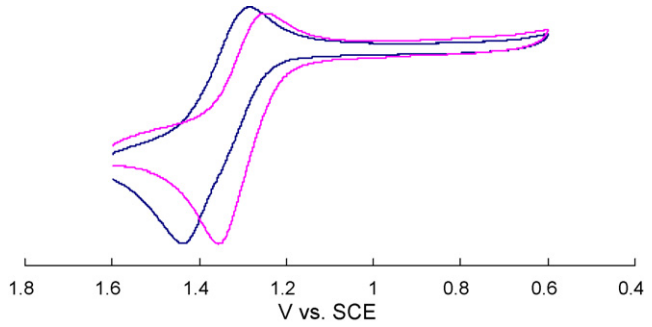

Fig. 5. Cyclic voltammetry of complex Ru-BL^5 (5×10^{-4} M) in CH_3CN (0.1 M TBAP) in the absence (blue) and presence (red) of Mg^{2+}. (For interpretation of the references to colour in this figure legend, the reader is referred to the web version of the article.)

Oxidation couple of complexes experienced a progressive cathodal shift upon addition of alkali and alkaline-earth metal ions to CH_3CN solution. After complete interaction, Ru(II)-centered $E_{1/2}$ of Ru-BL^2 and Ru-BL^5 (Fig. 5) exhibit the largest cathodal shift in the presence of Mg^{2+}, shifting from 1.308 and 1.362 V to 1.274 and 1.302 V respectively. Ru-BL^3 and Ru-BL^6 show the most cathodal shift in the presence of Ca^{2+}. Binding of cation introduces positive charge on the pseudocyclic polyether cavity. The positive charge may be partly delocalized over the whole bridging ligand framework, which increases the σ-donor and decreases the π-acceptor capacity of the ligand, resulting in destabilizing the dπ orbital of Ru(II). This facilitates the oxidation of Ru(II) by removal of an electron from dπ orbital of Ru(II).

According to the studies of UV–vis absorption, fluorescence, and cyclic voltammetry, Ru-BL^2 and Ru-BL^5 show the highest binding ability toward Mg^{2+} among five cations examined. It is considered that the ethylenedioxy bis(ethyleneoxy) tether in Ru-BL^2 and Ru-BL^5 can induce the most favorable conformation for the size-matched Li^+ (ionic diameter 1.36 Å) or Mg^{2+} (1.32 Å), while the difference between charge densities (1.47 qÅ^{-1} for Li^+, and 3.03 qÅ^{-1} for Mg^{2+}) leads to the large affinity only for Mg^{2+}. Based on the same reason, Ru-BL^3 and Ru-BL^6 prefer interacting with Ca^{2+} among the five cations examined.

5. Conclusions

Six polypyridyl bridging ligands and corresponding Ru(II) complexes have been prepared. Taking advantage of the character that some open-chain crown ether can selectively bind alkali and alkaline-earth metal ions, Li^+, Na^+, Mg^{2+}, Ca^{2+} and Ba^{2+} are added to the solution of Ru-BL$^{1-6}$, respectively. Alkali and alkaline-earth metal ions have no obvious modifying effect on the photophysical property of Ru-BL^1 and Ru-BL^4, but addition of metal ions to the solution of Ru-BL^{2,3,5,6} all result in a fluorescence quenching, a hyperchromic effect of the UV–vis absorption, and a progressive cathodal shift of Ru(II)-centered $E_{1/2}$. Ru-BL^2 and Ru-BL^5 show the highest binding ability toward Mg^{2+}, Ru-BL^3 and Ru-BL^6 exhibit selective recognition ability to Ca^{2+} among five cations examined. So Ru-BL^2 and Ru-BL^5 have potential utility as chemical sensor for probing Mg^{2+}, Ru-BL^3 and Ru-BL^6 can act as efficient chemical sensor for Ca^{2+}.

Synopsis

A new family of Ru(II) polypyridyl complexes Ru-BL$^{1-6}$ containing open-chain crown ether for Mg^{2+} and Ca^{2+} probing have been synthesized. According to the hyperchromic effect of UV-Vis absorption, fluorescence quenching, and cathodal shift of Ru(II)-centered $E_{1/2}$. Ru-BL^2 and Ru-BL^5 showed the response specific to Mg^{2+}; Ru-BL^3 and Ru-BL^6 showed selective recognition ability to Ca^{2+}.

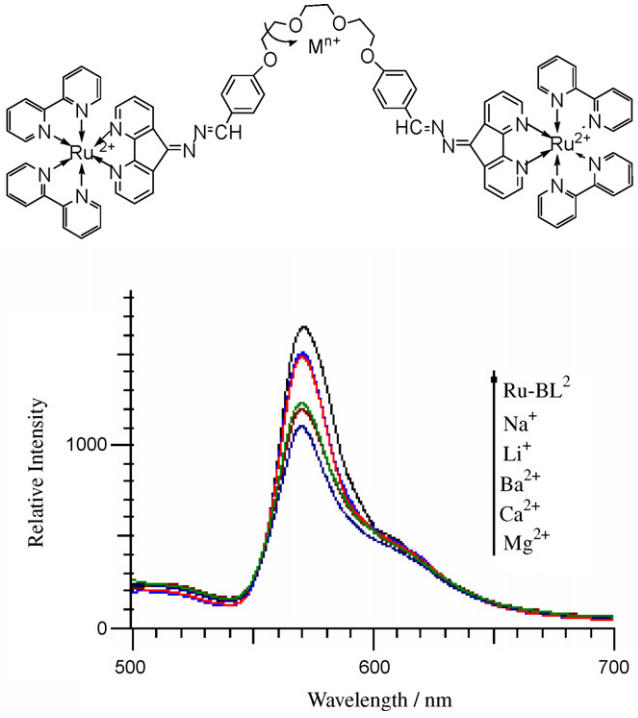

Acknowledgments

We are grateful to the National Natural Science Foundation of China (20571035) and the Gansu Natural Science Foundation of China (3ZS051-A25-003) for financial support.

Appendix A. Supplementary data

Supplementary data associated with this article can be found, in the online version, at doi:10.1016/j.saa.2008.07.031.

References

[1] A.A. Marti, C.A. Puckett, J. Dyer, N. Stevens, S. Jockusch, J. Ju, J.K. Barton, N.J. Turro, J. Am. Chem. Soc. 129 (2007) 8680.
[2] C.-F. Chow, B.K.W. Chiu, M.H.W. Lam, W.-Y. Wong, J. Am. Chem. Soc. 125 (2003) 7802.
[3] P.D. Beer, F. Szemes, P. Passaniti, M. Maestri, Inorg. Chem. 43 (2004) 3965.
[4] H.D. Batey, A.C. Whitwood, A.-K. Duhme-Klair, Inorg. Chem. 46 (2007) 6516.
[5] V. Amendola, L. Fabbrizzi, M. Licchelli, C. Mangano, P. Pallavicini, L. Parodi, A. Poggi, Coord. Chem. Rev. 190–192 (1999) 649.
[6] M. Schmittel, H. Lin, Inorg. Chem. 46 (2007) 9139.
[7] S. Mizukami, T. Nagano, Y. Urano, A. Odani, K. Kikuchi, J. Am. Chem. Soc. 124 (2002) 3920.
[8] A.P. de Silva, J. Wilers, G. Zlokarnik, Proc. Natl. Acad. Sci. U.S.A. 96 (1999) 8336.
[9] B. Valeur, I. Leray, Coord. Chem. Rev. 205 (2000) 3.
[10] K. Rurack, M. Kollmannsberger, U. Resch-Genger, J. Daub, J. Am. Chem. Soc. 122 (2000) 968.
[11] Y. Liu, A. Chouai, N.N. Degtyareva, D.A. Lutterman, K.R. Dunbar, C. Turro, J. Am. Chem. Soc. 127 (2005) 10796.
[12] A. Coskun, E.U. Akkaya, J. Am. Chem. Soc. 127 (2005) 10464.
[13] P. Bühlmann, E. Pretsch, E. Bakker, Chem. Rev. 98 (1998) 1593.
[14] L. Prodi, F. Bolletta, M. Montalti, N. Zaccheroni, Tetrahedron Lett. 39 (1998) 5451.
[15] R.A. Samant, V.S. Ijeri, A.K. Srivastava, J. Chem. Eng. Data 48 (2003) 203.
[16] S.P. Gromov, E.N. Ushakov, O.A. fedorova, I.I. Baskin, A.V. Buevich, E.N. Andryukhina, M.V. Alfimov, D. Johnels, U.G. Edlund, J.K. Whitesell, M.A. Fox, J. Org. Chem. 63 (2003) 6115.
[17] E. Arunkumar, P. Chithra, A. Ajayaghosh, J. Am. Chem. Soc. 126 (2004) 6590.
[18] A. Ajayaghosh, E. Arunkumar, J. Daub, Anger. Chem., Int. Ed. 41 (2002) 1766.
[19] L. Prodi, F. Bolletta, N. Zaccheroni, C.I.F. Watt, N.J. Mooney, Chem. Eur. J. 4 (1998) 1090.
[20] Y.-Z. Hu, Q. Xiang, R.P. Thummel, Inorg. Chem. 41 (2002) 3423.
[21] L.J. Charbonnière, R.F. Ziessel, C.A. Sams, A. Harriman, Inorg. Chem. 42 (2003) 3466.
[22] Y. Cui, H.-J. Mo, J.-C. Chen, Y.-L. Niu, Y.-R. Zhong, K.-C. Zheng, B.-H. Ye, Inorg. Chem. 46 (2007) 6427.
[23] M.E. Padilla-Tosta, J.M. Lloris, R. Martíner-Máñez, M.D. Marcos, M.A. Miranda, T. Pardo, F. Sancenón, J. Soto, Eur. J. Inorg. Chem. (2001) 1475.
[24] T. Lazarides, T.L. Easun, C. Veyne-Marti, W.Z. Alsindi, M.W. George, N. Deppermann, C.A. Hunter, H. Adams, H.W.D. Ward, J. Am. Chem. Soc. 129 (2007) 4014.
[25] Y. Liu, Z.-Y. Duan, H.-Y. Zhang, X.-L. Jiang, J.-P. Han, J. Org. Chem. 70 (2005) 1450.
[26] F. Gao, H. Chao, F. Zhou, B. Peng, L.N. Ji, Inorg. Chem. Commun. 10 (2007) 170.
[27] P. Anzenbacher Jr., D.S. Tyson, K. Jursíková, F.N. Castellano, J. Am. Chem. Soc. 124 (2002) 6232.
[28] P.D. Beer, S.W. Dent, Chem. Commun. (1998) 825.
[29] M.-J. Han, L.-H. Gao, Y.-Y. Lü, K.-Z. Wang, J. Phys. Chem. B 110 (2006) 2364.
[30] S. Sortino, S. Petralia, S. Di Bella, J. Am. Chem. Soc. 125 (2003) 5610.
[31] H.O. House, E. Feng, N.P. Peet, J. Org. Chem. 36 (1971) 2371.
[32] M.J. Plater, S. Kemp, E. Lattmann, J. Chem. Soc., Perkin. Trans. 1 (2000) 971.
[33] J. Mlochowski, Z. Szulc, Pol. J. Chem. 57 (1983) 33.
[34] M.B. Degtyareva, E.M. Demyanchuk, A.A. Simanova, Russ. J. Org. Chem. 41 (2005) 1690.
[35] R. Francesca, C.N. Di Bello, G. Doddi, V. Fares, P. Mencarelli, E. Ullucci, Tetrahedron 59 (2003) 9971.
[36] B.P. Sullivan, D.J. Salmon, T.J. Meyer, Inorg. Chem. 17 (1978) 3334.
[37] R.J. Watts, G.A. Crosby, J. Am. Chem. Soc. 94 (1972) 2606.
[38] Y. Wang, D.P. Rillema, Tetrahedron 53 (1997) 12377.
[39] Y. Wang, W.J. Perez, G.Y. Zheng, D.P. Rillema, C.L. Huber, Inorg. Chem. 37 (1998) 2227.
[40] Y. Wang, W. Perez, G.Y. Zheng, D.P. Rillema, Inorg. Chem. 37 (1998) 2051.
[41] J. Bolger, A. Gourdon, E. Ishow, J. Launay, Inorg. Chem. 35 (1996) 2937.
[42] P.T. Gulyas, T.A. Smith, M.N. Paddon-Row, J. Chem. Soc., Dalton Trans. (1999) 1325.
[43] A.K. Bilakhiya, B. Tyagi, P. Paul, Inorg. Chem. 41 (2002) 3830.
[44] N. Onozawa-Komatsuzaki, R. Katoh, Y. Himeda, H. Sugihara, H. Arakawa, K. Kasuga, Bull. Chem. Soc. Jpn. 76 (2003) 977.
[45] G.M. Brown, T.R. Weaver, F.R. Keene, T.J. Meyer, Inorg. Chem. 15 (1976) 190.
[46] V.W.-W. Yam, V.W.M. Lee, J. Chem. Soc., Dalton Trans. (1997) 3005.
[47] B.W.K. Chu, V.W.-W. Yam, Inorg. Chem. 40 (2001) 3324.
[48] D.P. Rillema, K.B. Mack, Inorg. Chem. 21 (1982) 3849.
[49] A. Juris, V. Balzani, F. Barigelletti, S. Campagna, P. Belser, A. von Zelewsky, Coord. Chem. Rev. 84 (1988) 85.
[50] W.M. Wacholtz, R.A. Auerbach, R.H. Schmehl, M. Ollino, W.R. Cherry, Inorg. Chem. 24 (1985) 1758.